Journal of the Korean Nuclear Society
Volume 17, Number 2, June 1985

《**Technical Report**》

An Effect of Energy Group Structure and Weighting Spectrum at the Resonance Energy Region of Iron on Neutron Shielding Calculation

Jung-Do Kim
Korea Advanced Energy Research Institute
Yukio Ishiguro
Japan Atomic Energy Research Institute
(Received February 2, 1985)

철의 공명에너지 영역의 에너지군구조 및 가중스펙트럼이 중성자 차폐계산에 미치는 영향

김 정 도
한국에너지연구소
이 시 구 로 유 끼 오
일본원자력연구소
(1985. 2. 2 접수)

Abstract

Effects of differences between fine- and broad-group structures and spectrum as a weighting function at the resonance energy region of iron on a neutron shielding calculation were analyzed with the ANISN code and ENDF/B-Ⅳ data. The problems analyzed are the broad-group effect, the effect for variation of iron thickness, and the effect of problem-dependent weighting spectrum.

In order to verify the group data and method used, a calculational benchmark was performed with the continuous-energy Monte Carlo code VIM. The result was compared with the ANISN calculations using the fine- and broad-group data.

요 약

중성자 차폐계산에 미치는 철의 공명에너지 영역에서의 미세군 및 소수군 구조에 의한 효과와 축약과정에서 사용되는 가중스펙트럼에 의한 효과를 ANISN 코드와 ENDF/B-Ⅳ자료로써 평가하였다. 다루어진 문제는 소수군효과, 철의 두께증가에 의한 영향 및 고려된 계를 대상으로한 미상군계산에서 얻은 스펙트럼을 사용한 군축약효과이다.

이용된 군정수와 코드의 정확성을 검토하기위해, 매우 정확한 계산정도를 갖고 있는 연속에너지 Monte Carlo코드 VIM에 의한 벤치마크계산을 수행하고 결과를 비교검토하였다.

1. Introduction

The neutron energy group structure of a multi-group cross-section library and the spectrum as a weighting function used in the process of generating the library are important factors, on the ground that they tend to result in considerable uncertainties in core or shielding calculations. It is well known that the resonance peak treatment of neutron cross-section is essential in the reactor neutronics problems, while the values of the resonance cross-section dip are more important than the peak values in the radiation shielding problems. Thus it is desired to have an adequate group structure at the resonance energy region of the shielding material.

In recent years, some fine-group libraries, i.e., those containing 100 or more neutron energy groups, are readily available as part of the Radiation Shielding Information Center's Data Library Collection (DLC)[1] of ORNL. In the energy group structure of the DLC-41/VITAMIN-C library,[2] for instance, the resonance peak and dip regions of sodium or iron are divided into more number of energy groups than those of the DLC-51/JSD-100 library.[3]

However, the expense of a fine-group approach in radiation shielding analysis usually makes it impractical for most users to exercise fine-group option. An alternative is to use a broad-group library collapsed from the fine-group ones using a problem-dependent spectrum as a weighting function.

In order to analyze the effects of differences between fine- and broad-group structures and weighting spectrum at the resonance energy region of iron on a practical shielding calculation, some neutron multi-group cross-section libraries were generated and the following problems were analyzed: 1) The effect of group structure, 2) the effect of iron thickness of the above problem, and 3) the effect of problem-dependent spectrum as a weighting function.

Moreover, in order to verify the adequacy of the multi-group cross-sections and the associated one-dimensional S_n-transport method, a calculational benchmark was performed using a continuous-energy Monte Carlo method.

The following section describes the calculational procedures. Section 3 discusses the results obtained in the calculations, whereas Section 4 summarizes some concluding remarks.

2. Calculational Procedures

2.1. Neutron Energy Group Structures

Three kinds of neutron energy group structures were adopted for the comparison of fine- and broad-group effects at the resonance energy region of iron on the neutron shielding calculations. The group structure of the DLC-23/CASK library[4] was adopted for the non-resonance energy region: the first eleven and the last seven groups cover the energy ranges from 14.9 to 1.108 MeV and from 583 to 10^{-5} eV, respectively. The remaining energy range from 1.108 MeV to 583 eV was divided into the same number of groups as the DLC-41/VITAMIN-C, DLC-51/JSD-100 and DLC-23/CASK libraries. Figure 1 shows some 22-group boundaries at the resonance energy region along with the total cross

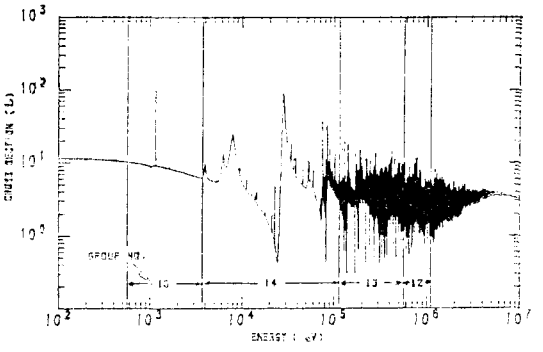

Fig. 1. Some 22-group Boundaries at the Resonance Energy Region and Total Cross-Sections of Iron in ENDF/B-IV

-section of iron from the ENDF/B-Ⅳ.[5]

2.2. Generation of Multi-group Cross-Sections

The 100-group (VIT-100G), 62-group (JSD-62G) and 22-group (CASK-22G) libraries were generated from the neutron data in ENDF/B-Ⅳ by using the SUPERTOG-JR3 routine in the code system RADHEAT-V3[6] with the option of 1/E plus fission spectrum weighting. All of the cross-sections are for 300°K. The hydrogen scattering data in the thermal energy region were processed with the free atom data in ENDF/B-Ⅳ, without considering the scattering law data of hydrogen bounded in water molecule.

2.3. Neutron Transport Calculation

As a model study, the neutron shielding design of a spent fuel shipping cask was examined. A one-dimensional cylindrical geometry was used to simplify the cask configuration. The dimensions and the compositions of the regions are given in Table 1 and 2, respectively.

Neutron transport calculations on the cask model were performed using the discrete ordinates code ANISN with a S_8-P_8 approximation. The typical mesh size in the lead and iron shield was about 1 cm. The source neutrons were assumed to have the uranium-235 fission spectrum. The neutron flux-to-dose conversion factors were calculated with the fitting equation given by the American National Standards Institute.[8]

Table 1. Cylindrical Cask Model Data

Region	Material	Outer Radius (inch)
1	Source	14.0
2	Stainless Steel	14.5
3	Coolant	17.0
4	Stainless Steel	17.5
5	Coolant	18.0
6	Stainless Steel	18.5
7	Lead	26.0
8	Stainless Steel	26.5
9	Air	29.5
10	Iron	33.0* (37.5)**

* 3.5-inch-thickness
** 8.0-inch-thickness

Table 2. Atom Number Densities of Materials Used in the Calculations

(10^{24} atoms/cm^3)

Material	Isotope	Concentration
Stainless Steel	Cr	1.65E-2*
	Fe	6.33E-2
	Ni	6.51E-3
Coolant	H	6.33E-2
	O	3.16E-2
Lead	Pb	3.25E-2
Air	N	4.13E-5
	O	9.04E-6
Iron	Fe	8.47E-2

* read as 1.65×10^{2}

2.4. Monte Carlo Calculation

The continuous-energy Monte Carlo code VIM[9] is available to provide efficient capability for the evaluation of multi-group cross-sections and calculational method as a calculational benchmark. In this code, the smooth cross-sections including the resolved resonances are specified pointwisely so that every point value can be determined by a linear interpolation. The unresolved resonances are presented by the method of probability table.[10] Neutron trajectories and scattering are continuous in angle. Anisotropic elastic and discrete level inelastic scattering are given with probability tables derived from the ENDF/B-Ⅳ data.

For a calculational benchmark, the neutron spectrum for the cask model with 8-inch-thick iron shield and the spectrum wieghted 22-group constant data were calculated by using the VIM code. The result was compared with the ANISN calculations using the fine- and broad-group libraries.

3. Results and Discussion

3.1. Broad-group Effect

The neutron dose rates for the modeled cask geometry calculated by using the three different

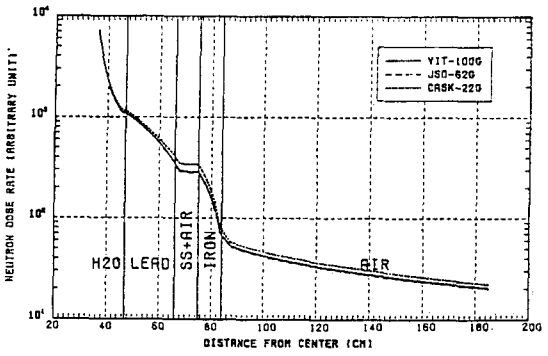

Fig. 2. Comparison of Neutron Dose Rate Distributions Calculated with Three Different Group Sets

group sets are plotted in Fig. 2. The figure shows good agreement between the results of VIT-100G and JSD-62G set in all the regions. The result using the CASK-22G broad-group set, however, shows higher values. At the position of 1 meter outside the cask surface, the result of CASK-22G set gives the higher dose rate by about 10% than those of both fine-group sets. After penetrating through the lead region, the calculated dose rates using the CASK-22G set are higher than those of the others.

The neutron dose rates in a resonance energy group between 3.35 and 111.1 keV are compared in Fig. 3. The neutron does rate in this energy range calculated with the CASK-22G set is rather underestimated at the outside of the cask

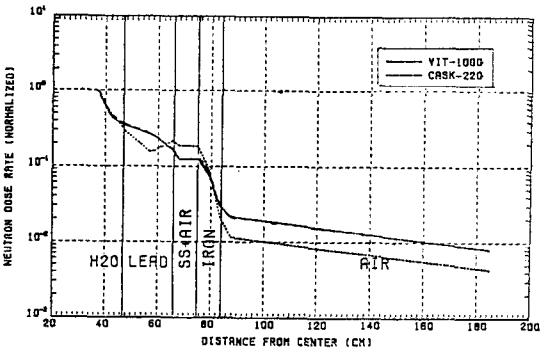

Fig. 3. Comparison of Neutron Dose Rate Distributions in the 3.35~111.09 keV Energy Range

surface in comparison with the fine-group results. This result may be explained as that the broad-group cross-sections collapsed with the 1/E weighting spectrum cannot reflect the effect of "iron window" correctly.

3.2. Effect of Iron Thickness

In order to survey an effect for the variation of iron thickness, a calculation for the case where the iron thickness is increased from 3.5 inches to 8.0 inches was performed by using the data and method. The result for the iron thickness of 8.0 inches is shown in Fig. 4. Compared to the result of the 3.5-inch-thick iron shield (Fig. 5), the result calculated with the CASK-22G set shows a flux build-up in the lead region while other two results decrease monotonically.

The neutron dose rate for the 8-inch-thick iron shield with the CASK-22G set gives a

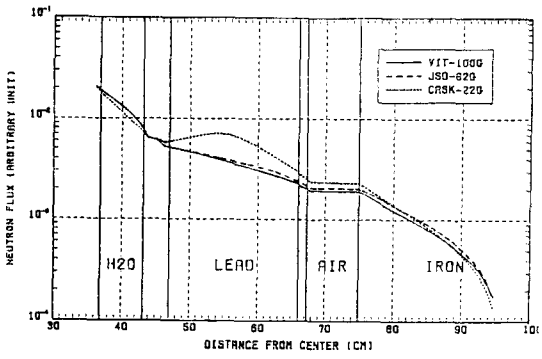

Fig. 4. Comparison of Total Neutron Flux Distributions for 8-inch-thick Iron Shield

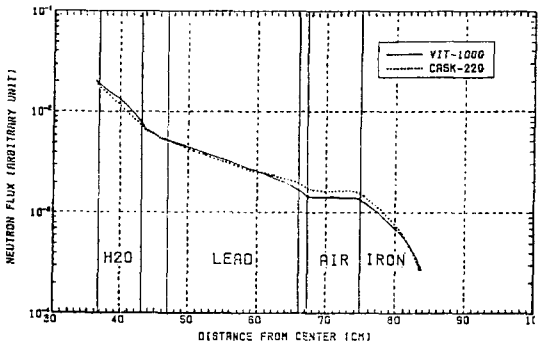

Fig. 5. Comparison of Total Neutron Flux Distributions for 3.5-inch-thick Iron Shield

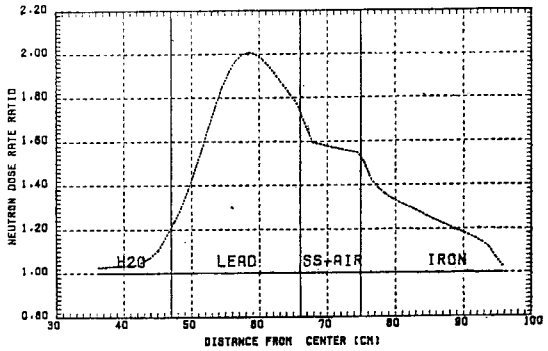

Fig. 6. Distribution of CASK-22G/VIT-100G Ratios of Neutron Dose Rate for 8-inch-thick Iron Shield

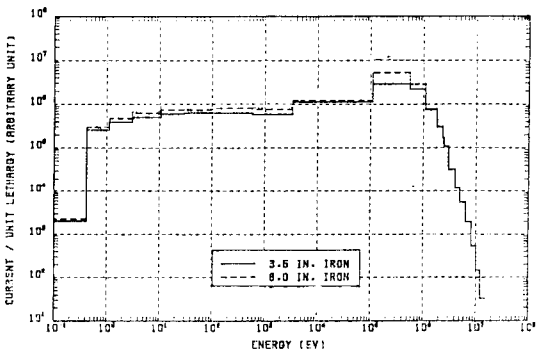

Fig. 7. Comparison of Neutron Currents emitted toward the Cask Center from the Inner Boundary of Iron

maximum of two times higher value in the lead region than that of the VIT-100G set(Fig. 6). The neutron current emitted toward the cask center from the inner boundary of the iron with the CASK-22G set increases with the iron thickness, and it is remarkable around the resonance energy region of iron(Fig. 7). These behaviors can be attributed to the drawback of the broad-group data of iron in the vicinity of the resonance energy region.

3.3. Problem-dependent Spectrum Weighting

In order to analyze the effect of the problem-dependent spectrum as a weighting function for collapsing the fine-group data, an advanced 22-group set(VICA-22G), which has the group structure of the CASK-22G set, was produced by collapsing the VIT-100G library using the ANISN spectrum at the center of the 8-inch-thick iron.

Figure 8 shows an improved result obtained from the VICA-22G set in comparison with the result of the CASK-22G set. An apparent improvement in the total neutron flux in the lead region for the increased iron shield was obtained by the revised broad-group data. This improvement may be mainly dependent on the revision of the group constant data in the resonance energy region of iron, since the iron total cross-section of the 14th group in the CASK-22G set is approximately two times

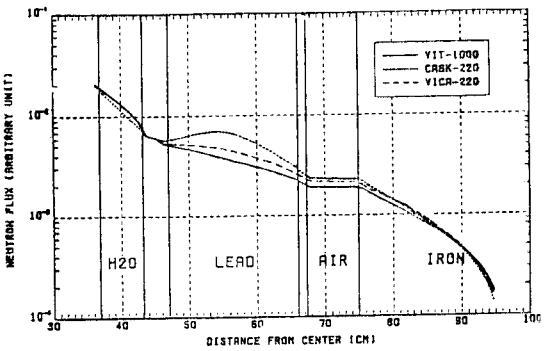

Fig. 8. Comparison of Total Neutron Flux Distributions Calculated with two Different 22-group Sets and a 100-group Set

Table 3. Comparison of 22-group Constant Data of Iron at the Resonance Energy Region

Group No.	Total Cross-Section (barns)		
	CASK-22G	VICA-22G	VIM
12	2.7903 (1.34)*	2.6102 (1.26)	2.0759
13	3.6959 (1.53)	3.3660 (1.39)	2.4146
14	8.0268 (2.13)	3.9833 (1.06)	3.7746
15	8.6371 (1.03)	8.3591 (0.99)	8.4193
Group No.	Capture Cross-Section (barns)		
	CASK-22G	VICA-22G	VIM
12	0.0042 (0.90)	0.0048 (1.01)	0.0047
13	0.0053 (0.98)	0.0055 (1.01)	0.0054
14	0.0140 (1.82)	0.0096 (1.25)	0.0077
15	0.1379 (3.93)	0.0989 (2.82)	0.0351

* ratio to VIM

larger than that of the VICA-22G set, as seen in Table 2.

3.4. Verification using Monte Carlo Method

As one of the calculational benchmarks, a Monte Carlo calculation was performed by using the continuous-energy Monte Carlo code VIM for the model with 8-inch-thick iron shield. The calculation was limited to a run of 100,000 histories.

Figure 9 shows the total flux distributions calculated by using the ANISN(VIT-100G) and the VIM code. The two results agree reasonably. The small overestimation of the ANISN flux in the lead region and the small underestimation in the iron may also be attributed to the multi-group constant set in the resonance energy region. Since the over-predicted elastic cross-sections in the vicinity of the resonance energy region of iron (see Table 2) will lead to a higher reflective property, the flux in the lead region might be increased. Conversely, the over-predicted capture cross-sections will lead to a decreasing flux in the iron region.

Table 2 shows some group constants for the resonance region in the 22-group sets generated by weighting three different spectra; the 1/E spectrum, ANISN and VIM spectra. It is noted that the CASK-22G and VICA-22G values are mostly larger than the values processed with the VIM.

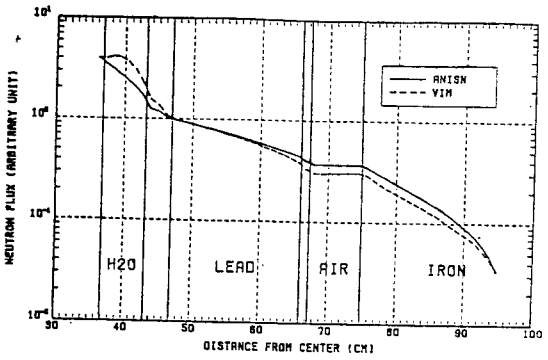

Fig. 9. Comparison of Total Neutron Flux Distributions Calculated with the ANISN(VIT-100G) and VIM code, respectively

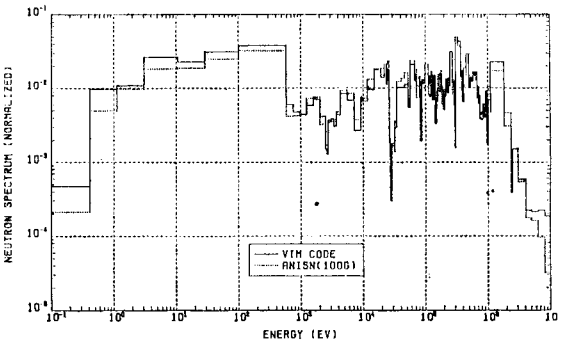

Fig. 10. Comparison of Neutron Spectra at the Middle Position of Iron Calculated with the ANISN(VIT-100G) and VIM code, respectively

In Fig. 9, the higher values in the water region would be caused by the inadequate treatment on the hydrogen data in the thermal energy region. In the VIM library, the hydrogen cross-sections are processed with the scattering law data of hydrogen bounded in water molecule.

In comparison with the result of the Monte Carlo calculation, the ANISN neutron spectrum at the middle position of iron calculated by using the VIT-100G set shows a good agreement (Fig. 10). However, it can be found that the ANISN results are somewhat higher than the other over the resonance energy region.

4. Concluding Remarks

In this report, the effects of fine- and broad-group structures and of spectrum as a weighting function at the resonance energy region of iron on the neutron shielding calculations were analyzed.

The result suggested that the broad-group prediction using 1/E spectrum weighting on the neutron shielding calculations for a shipping cask showed more or less conservative trend than those of fine-groups. A preferable agreement was seen between the JSD-62G and VIT-100G set.

According to the increase of the iron thickness, the total neutron flux calculated with the broad-group set, which was generated with the 1/E spectrum weighting, showed a tendency of flux build-up at the inside of the inner boundary of iron shield. On the other hand, an improvement on the above was obtained by using the broad-group set collapsed from the fine-group data with the problem-dependent ANISN spectrum weighting. This suggets that the weighting spectrum around the resonance energy region of iron is very sensitive to predict the neutron dose rate of iron shield. Therefore, in order to evaluate accurately the neutron dose rate for the iron shield using a broad-group library, it is essential to use a problem-dependent spectrum weighting at the resonance energy region for generating the broad-group cross-sections.

The broad-group cross-sections of iron prepared with the 1/E and ANISN spectrum always show a tendency of overestimate at the resonance energy region compared to the result of the calculational benchmark using the VIM code.

Acknowledgment

The authors wish to express many thanks to Dr. Takamasa MORI for his valuable discussions and helpful assistance in the use of the computer codes. Valuable comments by Dr. Masayuki NAKAGAWA are deeply appreciated. This work was performed in the most part at the Japan Atomic Energy Research Institute.

References

1. Proc. of a Specialists' Meeting on "Nuclear Data Benchmarks for Reactor Shielding", Paris(1980), p. 35.
2. R.W. Roussin, et al., "Experience in Developing and Using the VITAMIN-C 171-Neutron, 36-Gamma-Ray Multigroup Coupled Cross-Section Library", ORNL/RSIC-41 (1978), p. 107.
3. K. Koyama, et al., "Multigroup Cross-Section Sets for Shielding Materials -100 neutron groups and 20 gamma-ray groups in P_5 approximation-", JAERI-M 6928 (1977).
4. G.W. Morrison, et al., "A Coupled Neutron and Gamma-Ray Multigroup Cross-Section Library for Use in Shielding Calulations", Trans. Am. Nucl. Soc., 15, 535 (1972), DLC-23/CASK
5. D. Garber, "ENDF/B Summary Documentation", BNL-17451 (1975).
6. K. Koyama, et al., "RADHEAT-V3, A Code System for Generating Coupled Neutron and Gamma-Ray Group Constants and Analysing Radiation Transport", JAERI-M 7155 (1977).
7. W.W. Engle, Jr., "A User's Manual for ANISN, A One-Dimensional Discrete Ordinates Transport Code with Anisotropic Scattering", K-1693(1967).
8. "Neutron and Gamma-Ray Flux-to-Dose Rate Factors," ANSI/ANS-6.1.1-1977 (N666), American National Standards Institute (1977).
9. L.J. Milton, "VIM User's Guide", Argonne National Laboratory (1981).
10. L.B. Levitt, "The Probability Table Method for Treating Unresolved Resonances in Monte Carlo Criticality Calculations", Trans. Am. Nucl. Soc., 14, 684 (1971).